Motions in a Bose condensate. V. Stability of solitary wave solutions of non-linear Schrodinger equations in two and three dimensions

1986 J. Phys. A: Math. Gen. 19 2991

(http://iopscience.iop.org/0305-4470/19/15/023)

J. Phys. A: Math. Gen. 19 (1986) 2991-3011. Printed in Great Britain

Motions in a Bose condensate: V. Stability of solitary wave solutions of non-linear Schrödinger equations in two and three dimensions

C A Jones, S J Putterman† and P H Roberts‡

School of Mathematics, University of Newcastle upon Tyne, Newcastle upon Tyne NE1 7RU, UK

Received 3 December 1985

Abstract. The non-linear Schrödinger equation has previously been solved in two dimensions (2D) and three dimensions (3D) to give sequences of solitary waves, i.e. finite amplitude disturbances that propagate without change of form. The 3D dispersion relationship (the plot of energy, $\mathscr{E}$, against quasimomentum, p) has two branches for $p > p_{\min}$ and none for $p < p_{\min}$. The lower energy branch consists largely of disturbances possessing circulation and resembling large vortex rings in the limit $p \to \infty$. The upper energy branch consists of rarefaction pulses that are governed as $p \to \infty$ by the Kadomtsev-Petviashvili (KP) equation. The 2D dispersion relationship (where $\mathscr{E}$ and p refer to unit length) is a single branch of solitary waves extending from $p = 0$ to $p = \infty$, the latter resembling vortex pairs and the former being rarefaction pulses governed by the KP equation.

In this paper new integral properties of the solitary waves are derived, and are tested against previous numerical work. Their forms in the KP limit are compared with the results of Iordanskii and Smirnov.

The stability of solitary waves is examined both analytically and numerically. The analysis compares $\mathscr{E}$ for a solitary wave with $\mathscr{E}$ for a neighbouring state of the same p, obtained from a solitary wave by coordinate stretching. On this basis it is suggested that the lower branch of the 3D waves and the entire 2D sequence is stable to these disturbances, whereas the upper branch 3D solutions appear to be unstable. The implied creation of circulation if an upper branch solution descends in energy to a lower branch wave is examined, and is shown not to violate Kelvin's theorem. The tensor virial theorem is derived. Numerical work is presented that supports the analytical arguments.

1. Introduction

This paper is the fifth in a series of studies on the properties of the imperfect Bose condensate: see Roberts and Grant (1971, I), Grant (1971, II), Grant and Roberts (1974, III) and Jones and Roberts (1982, IV). In particular, it is a sequel to paper IV in which axisymmetric solitary waves were studied numerically. Such a wave is defined as a disturbance that moves through the fluid with speed U (say) preserving its form as it does so. The simplest example of such a disturbance was obtained for $U \to 0$ and closely resembles a classical vortex ring of circulation $\kappa = h/m$, where h is Planck's constant and m is the atomic mass.

† Permanent address: Physics Department, University of California, Los Angeles, CA 90024, USA.
‡ Now at: Mathematics Department, University of California, Los Angeles, CA 90024, USA.

0305-4470/86/152991+21$02.50

As U was increased, some unexpected and remarkable results emerged. The energy, $\mathscr{E}$, and (quasi-) momentum, p, of the wave at first diminished, as did the spatial scale of the disturbance, the cores at opposite sides of a diameter of the vortex tending to merge, so creating a region of depleted density throughout and around the entire vortex ring. Further increase of U led to loss of vorticity, at $p = p_V$ (say), but not to a loss of the solution. At first p and $\mathscr{E}$ continued to decrease, but then a cusp was reached in the $p\mathscr{E}$ plane at which p and $\mathscr{E}$ attained simultaneous minima, p_{min} and $\mathscr{E}_{min}$. Thereafter p and $\mathscr{E}$ increased (as did the spatial scale of the disturbance, which now formed a rarefaction pulse) until, as U approached the speed of sound, c, they became infinite. Thus for all $p > p_{min}$, the dispersion relationship for the solitary wave has two branches: a lower energy 'vortex' branch and a higher energy 'rarefaction' branch (see figure 1(a)).

On both upper and lower branches, solutions can be obtained in the limit $p \to \infty$ by asymptotic methods. This was done in paper I for the vortex branch and in the appendix to paper IV for the rarefaction branch. It was found that as $U \to c$, the rarefaction pulse was governed by a three-dimensional Kadomtsev-Petviashvili (1970) equation, and that it extended over distances of order a/ε along the symmetry axis (its direction of motion) and over distances of order a/ε^2 in the transverse directions. Here a is the healing length and $\varepsilon^2 = 1 - U/c$. The fluid velocity associated with the pulse is of order $\varepsilon^2 c$, and the deviation in the density from its undisturbed value, ρ_0, is of order $\varepsilon^2 \rho_0$. We have since learned that essentially the same asymptotic theory for the rarefaction pulse had earlier been given by Iordanskii and Smirnov (1978). They, however, did not suggest that the upper rarefaction branch was in any way related to the lower vortex branch. Whether the branches would remain connected if a more realistic model of helium II were adopted is a completely open question. There is, however, no doubt whatsoever that the Ginzberg-Pitaevskii equations (on which this series of papers rests) does link them together, and that this fact is of interest to those seeking to elucidate the properties of the non-linear Schrödinger equation (the 'NLS equation' as we shall term it).

The present paper was motivated by a number of questions left unanswered by paper IV, and by the need to relate our work more closely to that of Iordanskii and

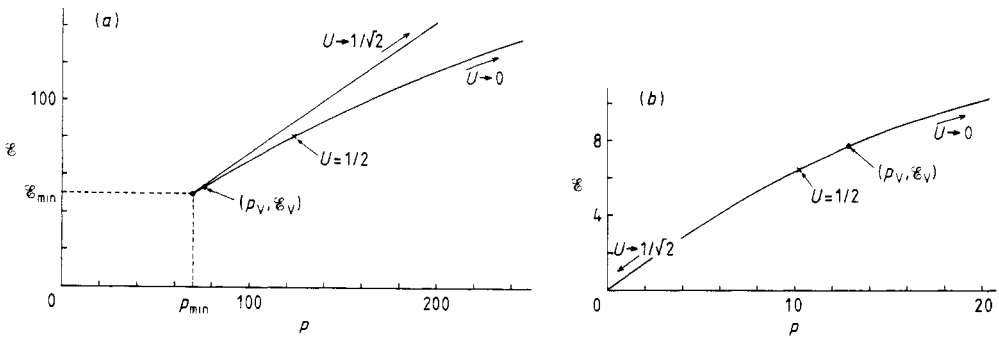

Figure 1. (a) The momentum, p, and energy $\mathscr{E}$ of the sequence of axisymmetric solitary wave solutions of the non-linear Schrödinger equation. The lower energy solutions possess vorticity for $p > p_V$, where $U \approx 0.62$. The remainder of that branch and the entire upper branch consists of rarefaction waves. The branches meet at the cusp (p_{min}, $\mathscr{E}_{min}$) at which $U \approx 0.657$. (b) The momentum per unit length, p, and the energy per unit length, $\mathscr{E}$, of the sequence of two-dimensional solitary wave solutions of the non-linear Schrödinger equation. For $p > p_V$, where $U \approx 0.43$, the solutions possess vorticity.

Smirnov (1978). It was, for instance, not immediately apparent that their result for the speed of the solitary wave was equivalent to ours. The new integrals needed to establish this are derived in § 2.

These new integrals were discovered while we were considering the relationship of our work to a theorem due to Derrick (1964; see also Lee 1981) on the non-existence of stable solitary waves in more than one spatial dimension. Later we discovered a way of deriving the new integrals directly. The way in which they bring our work into agreement with Iordanskii and Smirnov (1978) is discussed in § 3.

The NLS equation which results from the Bose condensate model can be written in scaled units as

$$-2\mathrm{i}\frac{\partial\Psi}{\partial t}=\nabla^2\Psi+\Psi(1-|\Psi|^2) \tag{1.1}$$

and must be solved subject to the boundary condition

$$\Psi\to 1 \qquad |\boldsymbol{x}|\to\infty \tag{1.2}$$

this applying for all directions of $\boldsymbol{x}$. Note that in many applications a slightly different NLS equation is considered in which the $1-|\Psi|^2$ term in (1.1) is replaced by $-|\Psi|^2$, and in which condition (1.2) is correspondingly replaced by $\Psi\to 0$, $|\boldsymbol{x}|\to\infty$ (see e.g. Ablowitz and Segur 1979). This 'zero boundary condition' problem gives rise to a rather different range of phenomena (e.g. see Christiansen and Lomdahl 1981).

By 'three-dimensional solitary waves' we will mean axisymmetric form-preserving solutions of (1.1) and (1.2), i.e.

$$\Psi=\Psi(s, z-Ut) \tag{1.3}$$

where (s, ϕ, z) are cylindrical coordinates. These evidently travel with velocity U in the z direction. Substituting (1.3) into (1.1) we have

$$2\mathrm{i}U\partial\Psi/\partial z=\nabla^2\Psi+\Psi(1-|\Psi|^2) \tag{1.4}$$

which we will solve for $t=0$. In addition to the three-dimensional (3D) solitary waves (1.3), we will also seek two-dimensional (2D) solutions of (1.1), i.e. solutions that are independent of one cartesian coordinate (y) and are also form-preserving:

$$\Psi=\Psi(x, z-Ut). \tag{1.5}$$

In the limit $U\to 0$ solutions (1.3) resemble classical vortex rings of circulation 2π, while solutions (1.5) become a pair of oppositely directed vortices of circulation 2π. The sequence of 2D solitary waves is shown in figure 1(b).

As mentioned above, an interesting feature of these sequences of solutions discovered in paper IV was the disappearance, as U was increased, of the zero of Ψ, which corresponds to the vortex core. This raises the question of whether it is possible for circulation to be created and destroyed during the time evolution of a solution of (1.1), or whether the Kelvin circulation theorem will prevent this from happening. This question is of some importance in the study of helium II and particularly in the study of superfluid turbulence (Barenghi *et al* 1983). It is discussed in § 4.

The last question we address is that of the stability of the solitary waves (1.3) and (1.5) shown in figure 1. This is a difficult problem and we have been unable to reach definite conclusions. On the basis of a number of arguments (§ 4), we conjecture that the 2D sequence of solitary waves found in paper IV is stable, as is the lower branch of the 3D solitary waves; the same arguments suggest that the upper branch of the

3D sequence is unstable. We also present results of some numerical computations of the time evolution of a finite difference scheme representing (1.1), and which are consistent with those conclusions.

We conclude this introduction by summarising some of the findings of paper IV that are relevant to this paper. It is well known that the flow at large distances from a classical vortex ring is dipolar. Analogously here, the solutions (1.3) to (1.4) have the form

$$\Psi \sim 1 - \frac{imz}{[z^2 + (1-2U^2)s^2]^{3/2}} + \ldots \qquad |\boldsymbol{x}| \to \infty. \tag{1.6}$$

Because of the factor $1-2U^2$, we term m 'the stretched dipole moment' of the wave. Similarly for solutions (1.5)

$$\Psi \sim 1 - \frac{imz}{[z^2 + (1-2U^2)x^2]} + \ldots \qquad |\boldsymbol{x}| \to \infty. \tag{1.7}$$

Because $U < 1/\sqrt{2}$ (the low frequency speed of sound), these forms do not give rise to unbounded Ψ. It was one of the objectives of paper IV to evaluate m for both 3D and 2D cases. The new integral relationships reported in § 2 provide new methods of evaluating m, and therefore of now subjecting the results to paper IV to *a posteriori* tests. These relationships also involve the momentum $\boldsymbol{p}$ and energy $\mathscr{E}$ of the waves:

$$\boldsymbol{p} = \frac{1}{2i} \int [(\Psi^* - 1)\nabla\Psi - (\Psi - 1)\nabla\Psi^*] \, dV \tag{1.8}$$

$$\mathscr{E} = \frac{1}{2} \int |\nabla\Psi|^2 \, dV + \frac{1}{4} \int (1 - |\Psi|^2)^2 \, dV \tag{1.9}$$

where $dV = s \, ds \, d\phi \, dz$ in the 3D case. In the 2D case, $\boldsymbol{p}$ and $\mathscr{E}$ are the momentum energy per unit y length and $dV = dx \, dz$. In both cases the integrals are taken over all space. It was shown in paper IV that, differentiating along the solitary wave sequences,

$$U = \partial\mathscr{E}/\partial p. \tag{1.10}$$

2. New integral properties

2.1. Three-dimensional solutions

Two integral properties were established in paper IV:

$$\mathscr{E} = Up + \tfrac{1}{4} \int (1 - |\Psi|^2)|1 - \Psi|^2 \, dV \tag{2.1}$$

$$4\pi m = p + \tfrac{1}{2}U \int (1 - |\Psi|^2)(2 - \Psi - \Psi^*) \, dV. \tag{2.2}$$

Two further integral relations were overlooked. Multiplying (1.4) by $\frac{1}{2}s\partial\Psi^*/\partial s$ taking the real part and integrating over all space, we obtain after some integrations by parts

$$2Up = \int \left|\frac{\partial\Psi}{\partial z}\right|^2 dV + \tfrac{1}{2} \int (1 - |\Psi|^2)^2 \, dV. \tag{2.3}$$

Similarly, multiplying (1.4) by $z\partial\Psi^*/\partial z$, we obtain

$$\int \left|\frac{\partial\Psi}{\partial z}\right|^2 \mathrm{d}V = \int |\nabla_{\mathrm{H}}\Psi|^2 \,\mathrm{d}V + \tfrac{1}{2}\int (1-|\Psi|^2)^2 \,\mathrm{d}V \tag{2.4}$$

where $\nabla_{\mathrm{H}} = \nabla - \hat{z}\partial/\partial z$ is the gradient perpendicular to $0z$. A number of further results follow from (1.8), (1.9) and (2.1)-(2.4). For example from (1.9) and (2.4)

$$\mathscr{E} = \int \left|\frac{\partial\Psi}{\partial z}\right|^2 \mathrm{d}V. \tag{2.5}$$

From (2.1), (2.3) and (2.5), we have

$$\mathscr{E} = \tfrac{1}{2}\int (1-|\Psi|^2)(2-\Psi-\Psi^*)\,\mathrm{d}V \tag{2.6}$$

$$Up = \tfrac{1}{4}\int (1-|\Psi|^2)(3-\Psi-\Psi^*-|\Psi|^2)\,\mathrm{d}V. \tag{2.7}$$

From (2.2) and (2.6) it follows that

$$4\pi m = p + U\mathscr{E}. \tag{2.8}$$

The last of these affords a new and immediate test of the numerical work of paper IV. Taking values listed in table 1 of that paper, we obtain table 1.

Table 1.

U	0.4	0.5	0.55	0.6	0.63	0.66	0.68	0.69
$4\pi m$	284	163	133	113	105	103	111	125
$p+U\mathscr{E}$	285	164	133	113	105	103	111	125

2.2. Two-dimensional solutions

With $\mathrm{d}V = \mathrm{d}x\,\mathrm{d}z$ and the different interpretations of $\mathscr{E}$ and p noted above, relation (2.1) holds as before. After correcting a misprint in (4.5) of paper IV, we have instead of (2.2)

$$2\pi m(1-2U^2)^{1/2} = p + \tfrac{1}{2}U\int (1-|\Psi|^2)(2-\Psi-\Psi^*)\,\mathrm{d}V. \tag{2.9}$$

To obtain the analogue of (2.3), we multiply (1.4) by $x\partial\Psi^*/\partial x$ and integrate over x and z, so obtaining

$$2Up = \int \left|\frac{\partial\Psi}{\partial z}\right|^2 \mathrm{d}V - \int \left|\frac{\partial\Psi}{\partial x}\right|^2 \mathrm{d}V + \tfrac{1}{2}\int (1-|\Psi|^2)^2\,\mathrm{d}V \tag{2.10}$$

while (2.4) and (2.5) require no change. Equations (2.6)-(2.8) have the following counterparts:

$$\mathscr{E} = \tfrac{1}{4}\int (1-|\Psi|^2)(3-\Psi-\Psi^*-|\Psi|^2)\,\mathrm{d}V \tag{2.11}$$

$$Up = \tfrac{1}{2}\int (1-|\Psi|^2)^2\,\mathrm{d}V \tag{2.12}$$

$$2\pi m(1-2U^2)^{1/2} = p(1-U^2) + 2U\mathscr{E}. \tag{2.13}$$

Taking values listed in table 2 of that paper, we obtain table 2 here.

Table 2.

U	0.3	0.4	0.5	0.6	0.65	0.68	0.69
$2\pi m(1-2U^2)^{1/2}$	23.8	18.4	14.0	9.68	7.03	4.88	3.89
$p(1-U^2)+2U\mathscr{E}$	23.8	18.4	14.0	9.68	7.02	4.88	3.89

3. The Kadomtsev–Petviashvili limits

3.1. Three-dimensional solutions

The form of the solution to (1.4) in the limit $U \to U_0$ (the speed of sound) was elucidated in the appendix to paper IV. Writing

$$\Psi = f + \mathrm{i}g \tag{3.1}$$

where f and g are real, we developed solutions for $\varepsilon \to 0$ of the form

$$f = 1 + \varepsilon^2 f_1 + \varepsilon^4 f_2 + \ldots \tag{3.2}$$

$$g = \varepsilon g_1 + \varepsilon^3 g_2 + \ldots \tag{3.3}$$

$$U = U_0 + \varepsilon^2 U_1 + \ldots \tag{3.4}$$

where f_i and g_i are functions of the stretched variables

$$\sigma = \varepsilon^2 s \qquad \zeta = \varepsilon z. \tag{3.5}$$

At leading order we showed, as expected, that

$$U_0 = 1/\sqrt{2} \tag{3.6}$$

and also that

$$f_1 = \frac{1}{\sqrt{2}} \frac{\partial g_1}{\partial \zeta} - \frac{1}{2} g_1^2. \tag{3.7}$$

To this order we also found that

$$\mathscr{E} = U_0 p \tag{3.8}$$

$$p = \tfrac{8}{3}\pi m \tag{3.9}$$

consistently with (1.10), (3.6) and (2.8). In terms of g_1, we obtained to the same accuracy

$$p = \frac{\sqrt{2}}{\varepsilon} \int \left(\frac{\partial g_1}{\partial \zeta} \right)^2 \mathrm{d}v \tag{3.10}$$

where $\mathrm{d}v = \varepsilon^5 \, \mathrm{d}V = 2\pi\sigma \, \mathrm{d}\sigma \, \mathrm{d}\zeta$.

Continuing to the next order, we discovered that g_1 obeyed the Kadomtsev-Petviashvili (1970) equation

$$2\sqrt{2} U_1 \frac{\partial^2 g_1}{\partial \zeta^2} - \nabla_{\mathrm{H}}^2 g_1 + \frac{\partial}{\partial \zeta} \left[\frac{1}{2} \frac{\partial^3 g_1}{\partial \zeta^3} - \frac{3}{\sqrt{2}} \left(\frac{\partial g_1}{\partial \zeta} \right)^2 \right] = 0 \tag{3.11}$$

where now $\nabla_{\mathrm{H}} = \nabla - \hat{z}\partial/\partial\zeta$, ∇ being defined from the stretched variables. Also, after some straightforward reductions, we may show from (2.1) that

$$\mathscr{E} = Up + K/p \tag{3.12}$$

where

$$K = -\frac{\varepsilon p}{2\sqrt{2}} \int \left(\frac{\partial g_1}{\partial \zeta}\right)^3 \mathrm{d}v = -\frac{1}{2} \int \left(\frac{\partial g_1}{\partial \zeta}\right)^3 \mathrm{d}v \int \left(\frac{\partial g_1}{\partial \zeta}\right)^2 \mathrm{d}v \tag{3.13}$$

the second form following from (3.10).

We are now able to expose the apparent contradiction with the similar analysis of Iordansky and Smirnov (1978) which we mentioned in § 1. These authors proposed (3.12) as the first two terms in the asymptotic expansion of $\mathscr{E}$ in the limit $p \to \infty$. Lacking (3.13), they evaluated the constant K as follows. By (1.8) the differential of (3.12) is

$$\mathrm{d}U/\mathrm{d}p = K/p^3. \tag{3.14}$$

Integrating this using (3.6) we obtain

$$U = 1/\sqrt{2} - K/2p^2 \tag{3.15}$$

so that by (3.4)

$$\varepsilon^2 U_1 = -K/2p^2 \tag{3.16}$$

or using (3.10)

$$K = -4U_1 \left[\int \left(\frac{\partial g_1}{\partial \zeta}\right)^2 \mathrm{d}v\right]^2. \tag{3.17}$$

Expressions (3.13) and (3.17) are consistent only if

$$2U_1 \int \left(\frac{\partial g_1}{\partial \zeta}\right)^2 \mathrm{d}v = \frac{1}{4} \int \left(\frac{\partial g_1}{\partial \zeta}\right)^3 \mathrm{d}v \tag{3.18}$$

a relationship that is far from apparent in the parent equation (3.11), and appeared at first to be possibly in contradiction with it.

Equation (3.18) follows directly from the new integral relations of § 2.1 after (3.1)-(3.4) have been inserted into them. Moreover, it is also found that

$$\sqrt{2} \int \left(\frac{\partial^2 g_1}{\partial \zeta^2}\right)^2 \mathrm{d}v + 3 \int \left(\frac{\partial g_1}{\partial \zeta}\right)^3 \mathrm{d}v = 0 \tag{3.19}$$

a second, far from obvious, result. Now it is clear, on multiplying (3.11) by $g_1 \, \mathrm{d}\zeta$ and integrating by parts, that

$$2\sqrt{2}U_1 \int \left(\frac{\partial g_1}{\partial \zeta}\right)^2 \mathrm{d}v = \int (\nabla_{\mathrm{H}} g_1)^2 \, \mathrm{d}v + \frac{1}{2} \int \left(\frac{\partial^2 g_1}{\partial \zeta^2}\right)^2 \mathrm{d}v + \frac{3}{\sqrt{2}} \int \left(\frac{\partial g_1}{\partial \zeta}\right)^3 \mathrm{d}v. \tag{3.20}$$

By (3.18) and (3.19) this implies

$$\int (\nabla_{\mathrm{H}} g_1)^2 \, \mathrm{d}v = -\frac{1}{\sqrt{2}} \int \left(\frac{\partial g_1}{\partial \zeta}\right)^3 \mathrm{d}v \tag{3.21}$$

and

$$2\sqrt{2}U_1 \int \left(\frac{\partial g_1}{\partial \zeta}\right)^2 \mathrm{d}v = -\tfrac{1}{2} \int (\nabla_{\mathrm{H}} g_1)^2 \, \mathrm{d}v \tag{3.22}$$

which shows that $U_1 < 0$; the wave moves subsonically. Also

$$K = \frac{1}{\sqrt{2}} \int \left(\frac{\partial g_1}{\partial \zeta}\right)^2 \mathrm{d}v \int (\nabla_{\mathrm{H}} g_1)^2 \, \mathrm{d}v \tag{3.23}$$

is evidently positive, i.e. $\mathrm{d}U/\mathrm{d}p > 0$ by (3.14).

3.2. Two-dimensional solutions

We may proceed with (3.1)-(3.4) as above in the two-dimensional case also, but now f_i and g_i are functions of the stretched variables

$$\xi = \varepsilon^2 x \qquad \zeta = \varepsilon z \tag{3.24}$$

and $dv = \varepsilon^3 \, dV = d\xi \, d\eta$. Since dV is $O(\varepsilon^{-3})$ rather than $O(\varepsilon^{-5})$, p is proportional (and not, as above, inversely proportional) to ε. While (3.6) and (3.8) hold as before, (3.9) and (3.10) are replaced by

$$p = 4\pi\varepsilon m/3 \tag{3.25}$$

$$p = \varepsilon\sqrt{2} \int \left(\frac{\partial g_1}{\partial \zeta}\right)^2 dv. \tag{3.26}$$

Equation (3.11) follows as before, while (2.1) gives in place of (3.12)

$$\mathscr{E} = Up + Kp^3 \tag{3.27}$$

where

$$K = -\frac{1}{2\sqrt{2}}\left(\frac{\varepsilon}{p}\right)^3 \int \left(\frac{\partial g_1}{\partial \zeta}\right)^3 dv = -\frac{1}{8} \int \left(\frac{\partial g_1}{\partial \zeta}\right)^3 dv \left[\int \left(\frac{\partial g_1}{\partial \zeta}\right)^2 dv\right]^{-3} \tag{3.28}$$

the second form following from (3.26).

Repeating the argument below (3.13), with the crucial difference that (3.27) is the asymptotic expansion for $p \to 0$, we have

$$dU/dp = -3Kp \tag{3.29}$$

which leads to

$$U = 1/\sqrt{2} - 3Kp^2/2 \tag{3.30}$$

and

$$\varepsilon^2 U_1 = -3Kp^2/2. \tag{3.31}$$

By (3.31) and (3.26) we have

$$K = -\tfrac{1}{3} U_1 \left[\int \left(\frac{\partial g_1}{\partial \zeta}\right)^2 dv\right]^{-2}. \tag{3.32}$$

Combining this with (3.28) we obtain instead of (3.18)

$$2U_1 \int \left(\frac{\partial g_1}{\partial \zeta}\right)^2 dv = \frac{3}{4} \int \left(\frac{\partial g_1}{\partial \zeta}\right)^3 dv. \tag{3.33}$$

Equation (3.33) follows directly from the new integral relations of § 2.2 after (3.1)-(3.4) have been inserted into them. It is the analogue of (3.18) while

$$\frac{1}{\sqrt{2}} \int \left(\frac{\partial^2 g_1}{\partial \zeta^2}\right)^2 dv + \int \left(\frac{\partial g_1}{\partial \zeta}\right)^3 dv = 0 \tag{3.34}$$

is the analogue of (3.19). Equation (3.20) holds as before, so that (3.21) and (3.22) are replaced by

$$\int (\nabla_H g_1)^2 \, dv = -\frac{1}{2\sqrt{2}} \int \left(\frac{\partial g_1}{\partial \zeta}\right)^3 dv \tag{3.35}$$

$$2\sqrt{2} U_1 \int \left(\frac{\partial g_1}{\partial \zeta}\right)^2 dv = -3 \int (\nabla_H g_1)^2 \, dv \tag{3.36}$$

which again shows that $U_1 < 0$. Also

$$K = \frac{1}{2\sqrt{2}} \int (\nabla_H g_1)^2 \, dv \left[\int \left(\frac{\partial g_1}{\partial \zeta} \right)^2 dv \right]^{-3} \tag{3.37}$$

is evidently positive, i.e. $dU/dp < 0$ by (3.29).

All these relations can be confirmed explicitly by using the exact solution of Manakov *et al* (1977):

$$U_1 = -\frac{1}{2\sqrt{2}} \qquad g_1 = -\frac{2\sqrt{2}\zeta}{\xi^2 + \zeta^2 + \frac{3}{2}} \tag{3.38}$$

and it is also found that

$$K = 3/128\pi^2\sqrt{2} \qquad m = 2\sqrt{2}. \tag{3.39}$$

4. Stability of solutions

4.1. General considerations

The stability of a solitary wave can sometimes be established by showing that it has minimum energy, $\mathscr{E}$, for given momentum, $\boldsymbol{p}$. Benjamin (1972) proved that the soliton solution of the one-dimensional (1D) KdV equation is stable by this method. The energy $\mathscr{E} = \mathscr{E}_0 + \Delta\mathscr{E}$, and momentum, $\boldsymbol{p} = \boldsymbol{p}_0 + \Delta\boldsymbol{p}$, of a state $\Psi = \Psi_0 + \Delta\Psi$ in the neighbourhood of a steady solitary wave state, Ψ_0, are in general different from the values $\mathscr{E}_0$ and $\boldsymbol{p}_0$ given by Ψ_0. Exceptional cases (excluded below) are disturbances $\Delta\Psi$ that merely correspond to rotation or translation of axes, for which $\Delta\mathscr{E}$ and Δp clearly vanish. Since Ψ_0 is itself only one member of a whole family of solitary waves on which p varies continuously, we can generally regard Ψ as a disturbance of a neighbouring solitary wave, $\Psi_0 + \Delta\Psi_0$, that has the same momentum $\boldsymbol{p}_0 + \Delta\boldsymbol{p}_0 = \boldsymbol{p}_0 + \Delta\boldsymbol{p}$. Taking this in place of Ψ_0 as the new reference state for Ψ, we may assume $\Delta\boldsymbol{p}$ is zero for $\Psi_0 + \Delta\Psi$. In general $\Delta\mathscr{E}$ will be non-zero. The sign of $\Delta\mathscr{E}$ is the central issue.

If $\Delta\mathscr{E} > 0$ for all sufficiently smooth $\Delta\Psi$ (such that $\Delta p = 0$) we may reasonably claim that the solitary wave is stable. Such a method of proof, requiring as it does every $\Delta\Psi$ to be considered, is not easily given: to show that $\Delta\mathscr{E} > 0$ for particular $\Delta\Psi$ establishes nothing.

From the fact that $\Delta\mathscr{E} < 0$ for one particular $\Delta\Psi$ one cannot, in the first instance, infer instability: $\boldsymbol{p}$ may not be the only constraint on the solutions. For instance Zakharov and Shabat (1973) found an infinite set of quantities conserved by the 1D NLS equation, of which p was only one. If the $\Psi_0 + \Delta\Psi$ giving negative $\Delta\mathscr{E}$ does not satisfy all these constraints, it is not accessible from Ψ_0, and it is therefore irrelevant to the stability of Ψ_0. Before instability can be claimed, it must be demonstrated that $\Psi_0 + \Delta\Psi$ obeys all constraints.

The only generalisation of the 1D NLS equation to 2D that is known to possess an infinite set of conservation laws is the Davey-Stewartson equation (Benney and Roskes 1969, Davey and Stewartson 1974) (see Anker and Freeman 1978). It does not seem to be possible to generalise the Zakharov-Shabat procedure to create conservation laws for our 2D and 3D NLS equations. The most plausible guess is that the multi-dimensional forms of (1.1) do not possess any additional conservation laws. There is no proof of this speculation at the present time, but we shall assume that it is true.

We might naturally be led to ask at this point whether the circulation

$$C(\Gamma)=\oint_{\Gamma} \boldsymbol{v}\cdot \mathrm{d}\boldsymbol{s} \qquad \boldsymbol{v}=\frac{1}{2\mathrm{i}}\left(\frac{1}{\Psi}\nabla\Psi-\frac{1}{\Psi^*}\nabla\Psi^*\right) \tag{4.1}$$

gives rise to further conservation laws. Single-valuedness of Ψ requires that $C(\Gamma)$ is zero if the curve Γ does not surround a curve (a 'vortex line') on which Ψ vanishes and is a multiple of 2π (in the present dimensionless units) if it does. The low velocity solitary waves possess vortex lines with circulation 2π corresponding to simple zeros of Ψ; the high velocity solitary waves do not. Especially for the 3D case, where one solution of each type exists for any sufficiently large p, the question naturally arises whether solutions with and without vorticity are accessible to one another. Classical fluid dynamics would suggest the answer, 'No'. If we adopt the Madelung transformation (see paper IV)

$$\Psi=R\exp(\mathrm{i}S) \qquad \rho=R^2 \qquad \boldsymbol{v}=\nabla S \tag{4.2}$$

we quickly find a parallel between (1.1) and the motion of a barotropic inviscid 'fluid' of density ρ, obeying the Kelvin-Helmholtz theorem of constancy of circulation $C(\Gamma)$ for all curves Γ moving with the fluid velocity $\boldsymbol{v}$. At first sight, then, it would seem again that states with and without circulation are inaccessible to each other. This however turns out not to be the case. It is a fact, borne out by the numerical conditions to be reported (see § 4.5), that, as Ψ evolves by (1.1), zeros can appear or disappear. As a vortex shrinks, any curve Γ which threads it is eventually brought to its 'core' (i.e. the curve on which ρ vanishes) at which instant Γ is no longer closed and Kelvin's theorem ceases to apply. We may however at the same instant define a new curve Γ', initially coincident with Γ, which is subsequently carried by the motion outside the ring, and round which (there being no enclosed zero of Ψ) the circulation $C(\Gamma')$ is zero.

These considerations suggest that it may be possible for solutions in the neighbourhood of the upper branch of the 3D solitary waves to collapse onto the lower branch, and in § 4.2 we give some support to the idea that the upper branch is indeed unstable. It is appropriate here to explain why our use of the word 'collapse' is appropriate. In Thomson's (1883) Adams' Prize Essay, two solitary waves (vortex rings) in an incompressible inviscid fluid were allowed to encounter one another, as a result exchanging energy and momentum but receding to infinity still 'ringing like bells'. We should emphasise that an encounter between two of our solitary waves would evolve differently. The 'ringing' set off by the 'collision' must, in a compressible medium, generate sound waves that radiate the excess energy in the ringing to infinity. Thus, in a coordinate frame moving with a stable solitary wave, the amplitude of a disturbance would, at any fixed point, ultimately approach zero. Thus, if a disturbed upper branch solution does evolve to the lower branch, the final state as $t\to\infty$ will be steady (in the comoving frame), the energy difference having been sonically radiated away. The word 'collapse' appears to describe this process aptly. In the language of stability theory 'collapse' implies that a stable solitary wave is also asymptotically stable, i.e. at every fixed point the disturbance disappears in time.

4.2. The Derrick-type arguments

One form of $\Psi_0+\Delta\Psi$ $(=\Psi)$ that satisfies the right conditions at infinity is, for the three-dimensional waves $(D=3)$,

$$\Psi=\Psi_0(as, bz) \tag{4.3}$$

or for the two-dimensional waves ($D=2$),

$$\Psi = \Psi_0(ax, bz) \tag{4.4}$$

where a and b are constants, which may be equal (Derrick 1964) but which are more dangerous for the stability of Ψ_0 when unequal. In fact the argument below, when generalised to arbitrary a and b, shows that the critical choice is $a \neq 1$, $b=1$, and we shall concentrate only on that case.

Referring to (1.8) and (1.9) we see at once that

$$\boldsymbol{p} = a^{1-D}\boldsymbol{p}_0 \tag{4.5}$$

and

$$\mathscr{E} = \tfrac{1}{2}a^{3-D}\int |\nabla_{\mathrm{H}}\Psi|^2 \,\mathrm{d}V + a^{1-D}\left(\frac{1}{2}\int \left|\frac{\partial\Psi}{\partial z}\right|^2 \mathrm{d}V + \frac{1}{4}\int (1-|\Psi|^2)^2 \,\mathrm{d}V\right) \tag{4.6}$$

or using the integral properties of § 2

$$\mathscr{E} = a^{1-D}[\mathscr{E}_0 + \tfrac{1}{2}(a^2-1)(D-1)(\mathscr{E}_0 - Up_0)]. \tag{4.7}$$

It is required to compare this with the energy of a solitary wave of momentum (4.5). Progress can be made when we limit ourselves to small deviations of a from unity, and work to second order in $a' = a-1$, an idea familiar from linear stability theory.

Let the solitary wave with momentum (4.5) have velocity $U+\delta U$. Correct to second order in δU we have

$$p - p_0 = \frac{\partial p_0}{\partial U}\delta U + \frac{1}{2}\frac{\partial^2 p_0}{\partial U^2}(\delta U)^2 \tag{4.8}$$

where the partial derivatives are taken along the solitary wave sequence at the state $a=1$. According to (4.5) the disturbance has momentum given by

$$p - p_0 = (1-D)p_0 a' - \tfrac{1}{2}D(1-D)p_0 a'^2 \tag{4.9}$$

to second order in a'. Equating (4.8) and (4.9) we determine, by the value of δU, the solitary wave having the same momentum as the disturbance

$$\delta U = \frac{(1-D)p_0 a'}{\partial p_0/\partial U} - \tfrac{1}{2}(1-D)\left(\frac{p_0 D}{\partial p_0/\partial U} + \frac{(1-D)p_0^2 \partial^2 p_0/\partial U^2}{(\partial p_0/\partial U)^3}\right)a'^2. \tag{4.10}$$

The corresponding energy of this solitary wave is $\mathscr{E}_0 + \delta\mathscr{E}_0$, where

$$\begin{aligned}\delta\mathscr{E}_0 &= \frac{\delta\mathscr{E}_0}{\partial U}\delta U + \frac{1}{2}\frac{\partial^2 \mathscr{E}_0}{\partial U^2}(\delta U)^2 \\ &= (1-D)\frac{p_0 \partial\mathscr{E}_0/\partial U}{\partial p_0/\partial U}a' - \tfrac{1}{2}(1-D) \\ &\quad \times\left[p_0 d\frac{\partial\mathscr{E}_0/\partial U}{\partial p_0/\partial U} - \frac{(1-D)p_0^2}{\partial p_0/\partial U}\frac{\partial}{\partial U}\left(\frac{\partial\mathscr{E}_0/\partial U}{\partial p_0/\partial U}\right)\right]a'^2 \\ &= (1-D)\{p_0 U a' - \tfrac{1}{2}[p_0 UD - (1-D)p_0^2 \partial U/\partial p_0]a'^2\}\end{aligned} \tag{4.11}$$

where in the last line we have used (1.10). The energy $\mathscr{E}_0 + \delta\mathscr{E}_0$ must be compared with the energy $\mathscr{E}_0 + \delta\mathscr{E}$ implied to order a'^2 by (4.7), which is

$$\delta\mathscr{E} = (1-D)\{p_0 U a' - \tfrac{1}{2}[\mathscr{E}_0 D + (3-2D)(\mathscr{E}_0 - Up_0)]a'^2\}. \tag{4.12}$$

The required energy difference is therefore

$$\Delta\mathscr{E} = \delta\mathscr{E} - \delta\mathscr{E}_0 = -\tfrac{1}{2}(D-1)[(D-3)(\mathscr{E} - Up) + (D-1)p^2\partial U/\partial p]a'^2 \tag{4.13}$$

in which we have omitted the zero suffix on the right, it being understood below that the expression is evaluated for the solitary waves themselves.

Since $\mathscr{E} > Up$ and $\partial U/\partial p < 0$ for the entire 2D sequence of solitary waves,

$$\Delta\mathscr{E} > 0 \qquad \text{for } D = 2. \tag{4.14}$$

From the reasons stated in § 4.1 this result proved for the single disturbance (4.4) establishes nothing.

On the lower branch of the 3D sequence of solitary waves, $\partial U/\partial p$ is negative; on the upper branch it is positive. Thus

$$\Delta\mathscr{E} > 0 \qquad \text{on lower branch } (D = 3) \tag{4.15L}$$

$$\Delta\mathscr{E} < 0 \qquad \text{on upper branch } (D = 3). \tag{4.15U}$$

Again we can conclude nothing about the stability of the lower branch, but if we accept the proviso of § 4.1, that no further conservation laws exist for the 3D NLS, we may conclude that the upper branch is unstable.

It appears also that the KP rational soliton, though stable in 2D (e.g. Freeman 1980), is unstable in three. It must be clearly recognised that these conclusions, like those of Derrick (1964), are crucially dependent on the assumed non-existence in two and three dimensions of additional conservation laws or other integrability constraints known to exist in one dimension for a variety of equations and in two dimensions for the Kadomtsev-Petviashvili equation.

4.3. Virial theorem

Information about solutions to (1.1) can be derived by the virial method (e.g. Chandrasekhar 1969). This has been successfully used to demonstrate self-focusing of 2D solutions to the NLS equations with zero boundary conditions, i.e with $|\Psi|^2$ replacing $|\Psi|^2 - 1$ in (1.1) and with $\Psi \to 0$ substituted for $\Psi \to 1$ in (1.2) (see Zakharov and Synakh 1976, Ablowitz and Segur 1979). The analogous results that apply in our case appear to be considerably less useful, but worth recording here.

The integral

$$M = \int (|\Psi|^2 - 1)\, \mathrm{d}V \tag{4.16}$$

is, like $\mathscr{E}$ and p, conserved by (1.1). Although convergent, its value for solitary waves depends on the shape of the 'surface at infinity', i.e. on the way that the $r \to \infty$ limit is taken in the integral: see (1.6) or (1.7). Such 'improper integrals' were discussed and interpreted in papers I and IV. If we take an initial Ψ in which the leading terms (1.6) or (1.7) in the large r expansion are absent, M is unambiguously defined. As this initial Ψ evolves, M is conserved. It may happen that, except at large r, a stable solitary wave develops, i.e. in a frame moving with the appropriate velocity, U, the disturbance approaches solitary wave form, except at large r. Nevertheless, at all sufficiently large r, transients will remain. If the integral (4.16) were performed over any large fixed volume in this frame, the answer would tend to a limit different from M, and this limit ($\tilde{M}$, say) would depend on the shape of that volume, being different

for (say) spheres or for rectangular boxes. The difference $M-\tilde{M}$ would refer to the still evolving solution outside that volume.

The integral (4.16) represents a mass defect initially established in the system ($|\Psi|^2$ is the normalised fluid density: see paper I). If $M \neq 0$, mass must have been added or subtracted when the disturbance was initiated It is reasonable to suppose, as we shall now do, that

$$M = 0 \tag{4.17}$$

i.e. the initial disturbance only displaces mass. (Non-zero M can also be removed by making an adjustment in the transformation to dimensionless variables: see paper I.)

The other integral of interest is the virial tensor

$$I_{ij} = \int x_i x_j (|\Psi|^2 - 1)\, \mathrm{d}V \tag{4.18}$$

which can be made finite by choosing the starting Ψ to lack stretched dipolar components, so that m as defined by (1.6) or (1.7) is zero initially. It can be shown from (1.1) that, if (4.16) holds,

$$\frac{\mathrm{d}^2 I_{ij}}{\mathrm{d}t^2} = \int \left(\frac{\partial \Psi}{\partial x_i}\frac{\partial \Psi^*}{\partial x_j} + \frac{\partial \Psi}{\partial x_j}\frac{\partial \Psi^*}{\partial x_i} \right) \mathrm{d}V + \tfrac{1}{2}\delta_{ij} \int (1-|\Psi|^2)^2\, \mathrm{d}V. \tag{4.19}$$

In particular

$$\frac{\mathrm{d}^2 I_{HH}}{\mathrm{d}t^2} = 2\int |\nabla_{\mathrm{H}}\Psi|^2\, \mathrm{d}V + \tfrac{1}{2}(D-1)\int (1-|\Psi|)^2\, \mathrm{d}V \tag{4.20H}$$

$$\frac{\mathrm{d}^2 I_{zz}}{\mathrm{d}t^2} = 2\int \left|\frac{\partial \Psi}{\partial z}\right|^2 \mathrm{d}V + \tfrac{1}{2}\int (1-|\Psi|^2)^2\, \mathrm{d}V \tag{4.20z}$$

and also

$$\frac{\mathrm{d}^2 I_{ii}}{\mathrm{d}t^2} = 4\mathscr{E} + \tfrac{1}{2}(D-2)\int (1-|\Psi|^2)^2\, \mathrm{d}V. \tag{4.21}$$

The fact that

$$I_{HH} \to +\infty \qquad I_{zz} \to +\infty \qquad t \to \infty \tag{4.22}$$

is consistent with the development of a dipole moment (1.6) or (1.7): in this context we should note that these asymptotic forms imply a positive density excess $|\Psi|^2 - 1$ at all sufficiently great distances, consistent with the development of a solitary wave or a number of solitary waves, and with the plus signs in (4.22). In the case $D = 2$, (4.21) can be integrated at once to give

$$I_{ii} = A + Bt + 2\mathscr{E}t^2$$

where A, B and $\mathscr{E}$ are constants.

4.4. Numerical evidence

To gain further insight into the stability of the solitary waves, a number of programs were written to solve the time-dependent 2D and 3D NLS (1.1). We sketch here only the essential points of the numerical techniques and present the results that seem most relevant.

In the axisymmetric 3D case, (1.1) takes the form

$$-2\mathrm{i}\frac{\partial\Psi}{\partial t}+2\mathrm{i}\,U_{\mathrm{F}}\frac{\partial\Psi}{\partial z}=\frac{1}{s}\frac{\partial}{\partial s}\left(s\frac{\partial\Psi}{\partial s}\right)+\frac{\partial^2\Psi}{\partial z^2}+\Psi(1-|\Psi|^2) \tag{4.23}$$

where $U_{\mathrm{F}}(>0)$, the velocity of the frame of reference, is chosen to retain the main disturbance in the centre of the frame. Initially the most appropriate value of U_{F} for the chosen initial state is unknown, but it can be found by trial and error. In cases where the initial disturbance breaks up into several solitary waves, all moving with different speeds, it is practicable to follow the time development of only one of them.

Solutions to (4.23) are required on infinite s and z intervals, a difficulty we met by transforming those coordinates to finite intervals by the stretching

$$\tilde{s}=\frac{s}{3+s}\qquad\tilde{z}=\frac{2}{\pi}\tan^{-1}\frac{z}{3} \tag{4.24}$$

which was found by trial to be satisfactory. The intervals $0\leqslant s\leqslant\infty$, $-\infty\leqslant z\leqslant\infty$ are now mapped into the finite box $0\leqslant\tilde{s}\leqslant 1$, $-1\leqslant\tilde{z}\leqslant 1$, which was represented by an equally spaced mesh, using up to 33×65 grid points. Time evolution was followed with the hopscotch method (Eilbeck 1978, Makhankov *et al* 1981) which is of second-order accuracy. The spatial derivatives were replaced by second-order centred differences.

The momentum and energy were evaluated inside a set of nested boxes centred on $\tilde{s}=\tilde{z}=0$, the last box embracing the entire system. In this way the spatial distributions of these quantities could be continuously monitored.

This scheme allowed reliable integrations for times of up to about $t=30$. Beyond this, a significant amount of energy is present at the outermost points of the grid, where stretching of coordinates is necessarily large. The accuracy of the representation then breaks down and the solution ceases to be reliable. Ideally, one would allow the outgoing radiation to escape from the box. Unfortunately in a dispersive medium such as this there is no simple way of imposing a local Sommerfeld condition. Simple attempts to cut the boundary off, or to add an artificial viscosity near the boundary, resulted in reflected waves that prevented the system from attaining a steady state. This problem has been recognised in a number of situations, and a discussion of various methods of alleviating the difficulty is given in Israeli and Orszag (1981). Because of these problems it is hard to rule out the possibility that solutions which appear stable over the time of integration are unstable to very slowly growing perturbations. Despite these difficulties, a number of interesting observations did emerge from the numerical integrations.

In the first case considered the initial momentum and energy were chosen to be below the critical values $p_{\min}$, $\mathscr{E}_{\min}$ (see figure 1(*a*)). The initial state, Ψ_{init}, was constructed from a steady-state solution Ψ_0, near the cusp (the $U=0.65$ steady solution, in fact) by writing

$$\Psi_{\mathrm{init}}=1+0.8(\Psi_0-1).$$

This gave an initial momentum and energy of 45.3 and 34.7, respectively. Figure 2 shows how the momentum and energy in a small box ($0\leqslant s\leqslant 3$, $-3\leqslant z\leqslant 3$) and in a larger box ($0\leqslant s\leqslant 5$, $-4.49\leqslant z\leqslant 4.49$) evolved in time; we denote these by p_{S}, $\mathscr{E}_{\mathrm{S}}$ for the small box, and p_{L}, $\mathscr{E}_{\mathrm{L}}$ for the large box. The total momentum and energy in the system are conserved, so the observed decay in p_{S}, $\mathscr{E}_{\mathrm{S}}$, p_{L}, $\mathscr{E}_{\mathrm{L}}$ is balanced by energy

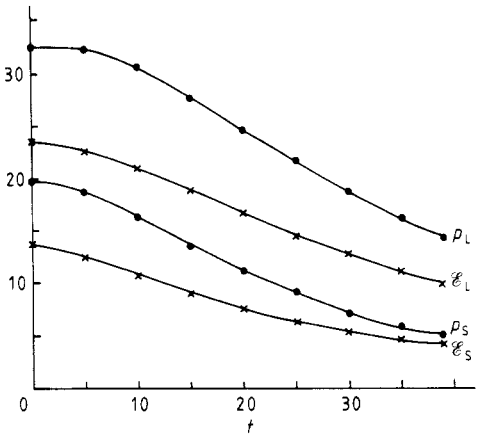

Figure 2. Time evolution of the momentum energy of an axisymmetric solution of the non-linear Schrödinger equation having $p = 45.3$, $\mathscr{E} = 34.7$. The $(p_S, \mathscr{E}_S)$ refer to integrals over the small control box $(0 \leq s \leq 3, |z| \leq 3)$, and the $(p_L, \mathscr{E}_L)$ refer to the same integrals over the large control box $(0 \leq s \leq 5, |z| \leq 4.49)$. The starting momentum and energy lie below the minimum values $(p_{min}, \mathscr{E}_{min})$: see figure 1(*a*). The solution appears to be evanescing.

radiated out of the boxes by sound waves. Figure 2 gives some idea of the timescale over which the solution may be expected to collapse completely.

In figure 3 we give corresponding diagrams for our second case in which

$$\Psi_{init} = 1 + (\Psi_0 - 1)[1 + 2\tilde{z}\exp(-0.3\tilde{z})]$$

where Ψ_0 is now the wave with $U = 0.5$, comfortably on the lower branch of figure 1(*a*). The evolutions of p_S, $\mathscr{E}_S$, p_L, $\mathscr{E}_L$ are quite different from those of figure 2. There is no evidence that the initial disturbance will evanesce into sound waves. Rather, the

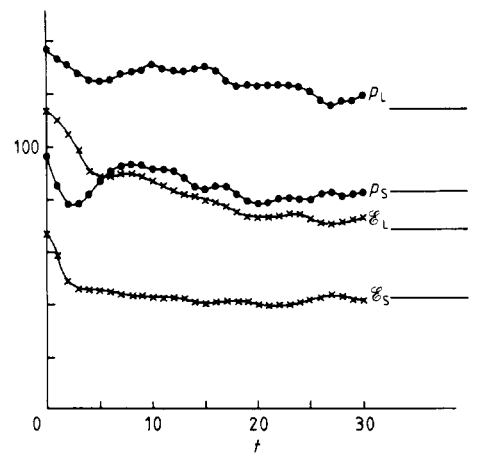

Figure 3. Time evolution of $(p_S, \mathscr{E}_S)$, $(p_L, \mathscr{E}_L)$ as defined in the caption of figure 2 for an axisymmetric solution of the non-linear Schrödinger equation having $p = 155.23$, $\mathscr{E} = 144.59$. The asymptotes to which these would tend if the solution became the $U = 0.5$ solitary wave are indicated by the horizontal lines on the right ($p_S \approx 83.677$, $\mathscr{E}_S \approx 42.606$, $p_L \approx 114.10$, $\mathscr{E}_L \approx 69.00$).

momenta and energies appear to stabilise at values near those expected for the $U = 0.5$ wave, and these are also shown on the right of figure 3. The final 'terminal' velocity, U_F, that retained the disturbance in the centre of the frame was also close to 0.5.

Figure 4 presents similar results for a solution of the 2D NLS. The numerical attack was almost identical to the one adopted above and the difficulties were very similar. The equation replacing (4.23) is

$$-2i\frac{\partial \Psi}{\partial t} + 2iU_F\frac{\partial \Psi}{\partial z} = \frac{\partial^2 \Psi}{\partial x^2} + \frac{\partial^2 \Psi}{\partial z^2} + \Psi(1 - |\Psi|^2) \tag{4.25}$$

and stretching (4.24) was again used (with $\tilde{s}$ and s replaced by $\tilde{x}$ and x). The solitary waves have no upper and lower branch and no minimum p and $\mathscr{E}$; there is therefore no analogue of the first case above. We constructed an analogue to the second case from

$$\Psi_{\text{init}} = 1 + (\Psi_0 - 1)[1 + \tilde{z}\exp(-0.3\tilde{z})]$$

where Ψ_0 was again for the $U = 0.5$ solitary wave. The plots of p_S, $\mathscr{E}_S$, p_L, $\mathscr{E}_L$ in figure 4 are again consistent with an approach to a steady state near $U = 0.5$.

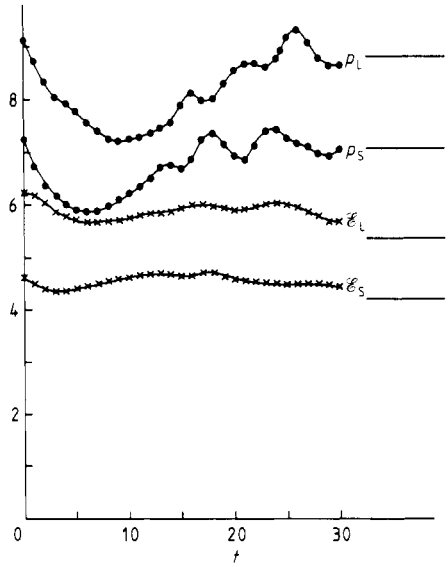

Figure 4. Time evolution of $(p_S, \mathscr{E}_S)$, $(p_L, \mathscr{E}_L)$ for a two-dimensional solution of the non-linear Schrödinger equation having $p = 10.67$, $\mathscr{E} = 8.46$. The control boxes are now $(0 \leq x \leq 3, |z| \leq 3)$ and $(0 \leq x \leq 5, |z| \leq 4.49)$. The asymptotes to which these would tend if the solution became the $U = 0.5$ solitary wave are indicated by the horizontal lines on the right ($p_S \approx 7.06$, $\mathscr{E}_S \approx 4.22$, $p_L \approx 8.813$, $\mathscr{E}_L \approx 5.375$).

Some of the oscillations of the p curves in figure 4 (and to a lesser extent in figure 3) are presumably due to reflection of waves from the sidewalls; although this effect has been reduced by the stretched mesh, it was not possible to eliminate it entirely. The experiments nevertheless suggest that the initial states corresponding to figures 3 and 4 settle down to the computed steady-state values, and do not completely decay away into radiation. As already mentioned, however, we cannot rule out by these numerical calculations the possibility of decay on a very long timescale.

4.5. Creation and destruction of circulation

We mentioned in § 4.1 that Kelvin's circulation theorem does not appear to impose a strong constraint on the evolution of solutions to the 2D and 3D NLS. In particular, it is possible in three dimensions for a simple zero of $\Psi(s, z)$, corresponding to a vortex ring, to appear naturally during the course of a time integration of (1.1): similarly the evolution of two-dimensional solutions can create a simple zero of $\Psi(x, z)$ corresponding to a vortex pair.

In figure 5, we show the time evolution of an initial state by means of contour plots of the scaled density $|\Psi|^2$. The initial state was a three-dimensional solution with no zero of Ψ and hence with no 'vorticity'. It was in fact constructed from a Derrick-type perturbation (4.3)

$$\Psi_{\text{init}} = \Psi_0(as, z) \qquad a = \tfrac{3}{8}$$

where Ψ_0 was the solitary wave for $U = 0.65$. The density contours are equally spaced at intervals of 0.1, the tenth contour line marking a density equal to that of the ambient medium. Successive pictures form a time sequence at intervals of $\Delta t = 2$. The contours were transformed back to the real physical coordinates (s, z) in the box $0 \leqslant s \leqslant 15$, $-10 \leqslant z \leqslant 10$. The initial momentum and energy were 503.5 and 331.4. The choice $U_F = 0.6$ of reference frame velocity was an appropriate compromise between the higher speed of the high density regions and the lower speed of the low density regions (and vortex 'core') which move to the bottom of the display window.

Until about $t = 14$, the minimum density occurs on the axis of symmetry and is greater than zero. Between $t = 14$ and $t = 16$ the innermost contour 'pinches off' the axis and forms a core surrounding a zero in density, $|\Psi(s, z)|^2$, corresponding to a vortex ring. As t increases, the core moves outwards, at first rapidly but subsequently increasingly slowly as it stabilises into a permanent structure. In short, between $t = 14$ and $t = 16$ a vortex ring has been created from an initial state that possessed no 'vorticity'. Similar events can be discussed in integrations of the 2D NLS, where a vortex pair may be produced from an initial configuration that had none. We consider this case further below.

We attempt to model the formation of a vortex pair at the origin at time $t = 0$. We shall focus on $C(\Gamma)$ for the curve Γ shown in figure 6, in which the location of the vortex pair at small positive t is marked by crossses. Since the fluid 'velocity' (4.1) on the axis of symmetry $0z$ is always directed along the axis, the segment Γ_1 of Γ is a material curve throughout. The semicircular segment Γ_2 at infinity may move slightly, but because of its remoteness its contribution to the circulation will scarcely alter. The same will be true on Γ_1 except near the origin, and we show in figure 6 an imaginary (broken) circle containing the only part, Γ_{10}, of Γ, on which significant changes occur during the creation of the vortex pair.

Provided $|x| = O(\varepsilon^{1/2})$ and $|z| = O(\varepsilon)$, Ψ may be approximated by

$$\Psi = aU_F(\varepsilon - x^2) + ca(z - U_F v_0 x^2) \tag{4.26}$$

where $\varepsilon = v_0 t$ is small in modulus, i.e. we consider only very small times before and after the instant at which the vortex pair is created; a and v_0 are constants. Substituting into (4.25) we see that (4.26) is a solution to leading order in ε, i.e. it is locally valid near 0.

For $t < 0$, the Ψ of (4.26) has no zeros near 0 nor (as we shall suppose) far from 0. Since $\Psi = R \exp(iS)$ is single-valued, so is S, and the circulation (4.1) vanishes for

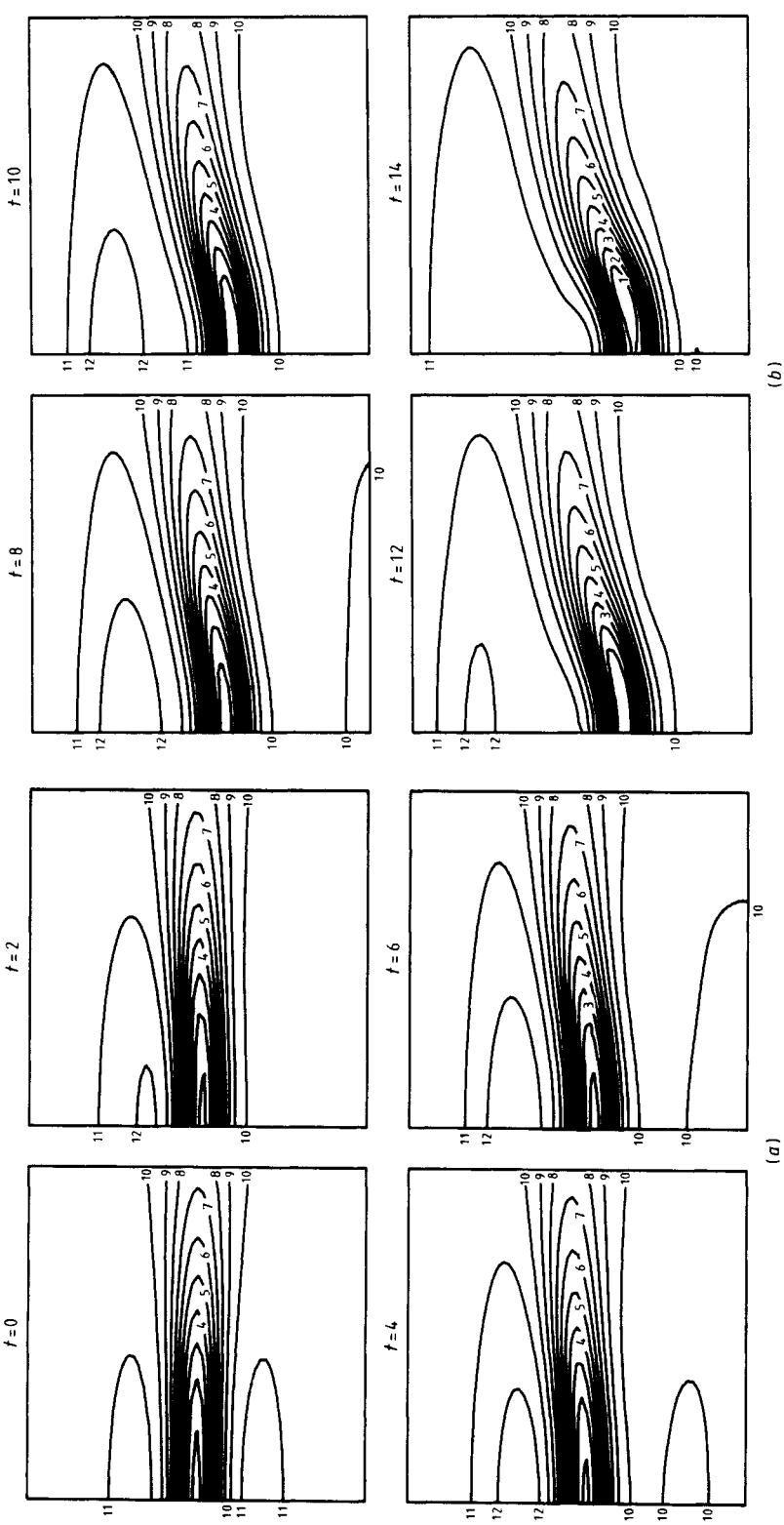

Figure 5. Equidensity plots of the density $|\Psi|^2$ for $t = 0, 2, \ldots, 22$ for the time evolution of an axisymmetric solution of the non-linear Schrödinger equation starting from a disturbed state ($U \approx 0.65$) of a solitary wave on the upper branch of figure 1(*a*). It will be seen that a vortex core establishes itself over the sequence. The number n on a contour line indicates that the density is $(n/10)$ times the ambient density of the undisturbed state ($\Psi = 1$).

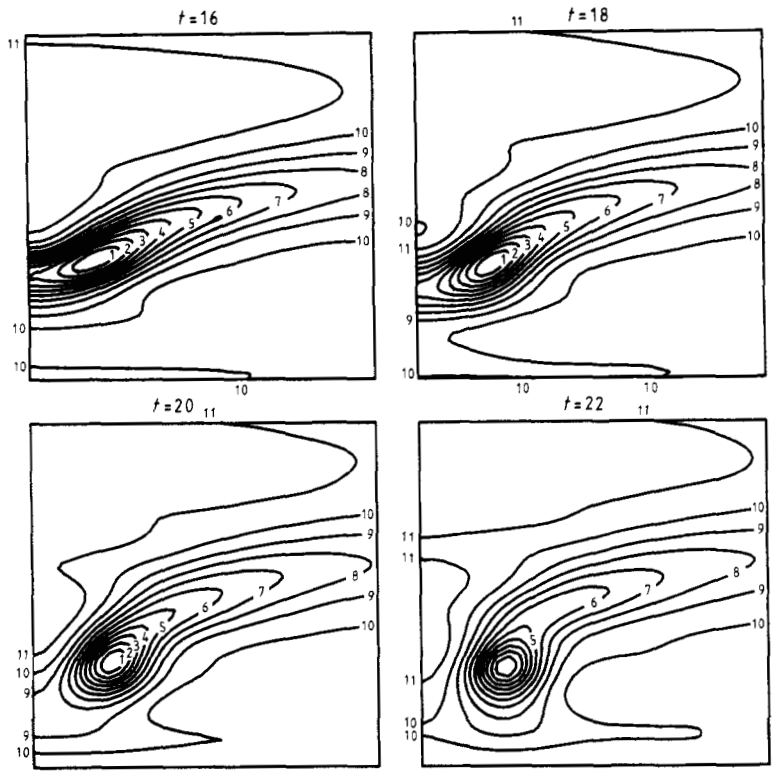

Figure 5. (continued)

all curves, including Γ. We may note however that as t approaches 0, the 'fluid velocity' on Γ_{10},

$$v_z = \frac{\varepsilon U_F}{(\varepsilon U_F)^2 + z^2} \tag{4.27}$$

becomes very large at 0 while the density in (4.2)

$$\rho = a^2[(\varepsilon U_F)^2 + z^2] \tag{4.28}$$

tends to zero equally rapidly, their product (the momentum density) being finite and vanishing at $t = 0$. Because of the size of v_z, the segment Γ_{10} makes a significant contribution to $C(\Gamma)$.

For $t > 0$, the Ψ of (4.26) is single-valued but, since it has acquired two zeros $x = \pm\varepsilon^{1/2} = \pm(v_0 t)^{1/2}$, $z = U_F v_0^2 t$, S is not. The velocity, still given by (4.27) near 0, is reversed, as is the contribution to the circulation from Γ_{10}, i.e.

$$C(\Gamma_{10}) = \int_{-\infty}^{\infty} \frac{\varepsilon U_F \, dz}{(\varepsilon U_F)^2 + z^2} = \begin{cases} \pi & \text{if } \varepsilon > 0 \\ -\pi & \text{if } \varepsilon < 0. \end{cases} \tag{4.29}$$

Since the total circulation was zero for $t < 0$, the segment ABCDE (figure 6) must make the contribution π throughout, so that for $t > 0$ the net circulation is 2π by (4.29).

We may wonder what happens at $t = 0$ itself when (4.29) is meaningless. At this moment a zero of ρ lies on Γ. Lacking 'material' at 0 it can scarcely be described as

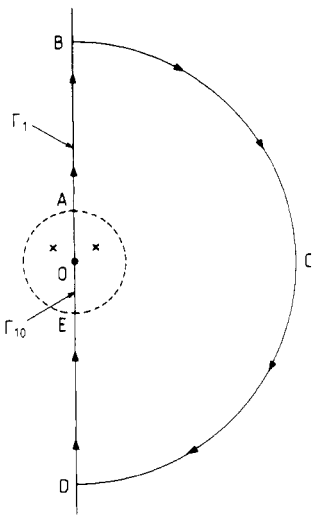

Figure 6. Schematic figure illustrating the application of Kelvin's theorem to the contour ABCDEOA for a two-dimensional solution of the non-linear Schrödinger equation in a case when a vortex pair (marked with XX) appears at $t = 0$. For a further description, see text.

a 'material curve' in the sense of Kelvin's theorem. Stated another way, Γ ceases to be a closed curve at $t = 0$. We may if we wish define a new material curve, Γ', coincident with Γ at that instant and subsequently passing between the vortex pair, but the circulation $C(\Gamma')$ will differ from $C(\Gamma)$ by 2π.

Through model (4.26) we have been able to show how circulation may be created without the appearance of any singular behaviour in Ψ. It is presumably also possibly by reversing the sign of v_0 in model (4.26) to destroy vorticity, and indeed the NLS equation is time-reversible: $t \to -t$, $\Psi \to \Psi^*$. When considering the stability of solitary waves, such transformations are however inadmissible since they ignore an important ingredient: the fact that a disturbed solitary wave radiates sound away from it and not towards it. Stability questions are not time-reversible when the Sommerfeld condition is properly included.

5. Conclusions

The first part of this paper has been devoted to the derivation of new integral properties of solitary waves in both two and three dimensions, and in using these to test the numerical work of paper IV; tables 1 and 2 display the resulting vindication of those integrations. In § 3 the new integrals were specialised to the KP limit in which the speed of the solitary waves approach that of low frequency sound ($2^{-1/2}$). This allowed us to bring our theory into harmony with that of Iordanskii and Smirnov (1978).

The main part of the paper (§ 4) was concerned with the stability of the solitary waves. Attention was focused on axisymmetric disturbances of the 3D waves, and on two-dimensional distortions of the 2D waves. The analytic approach was hampered by uncertainty to whether the 2D and 3D forms of the NLS equation possess (as the 1D form is known to do) an infinite sequence of conservation laws. Assuming that only

p and $\mathscr{E}$ are conserved in two and three dimensions, we could show that the upper branch of the 3D sequence is unstable. We did this by proving that, in the neighbourhood of any state $(p, \mathscr{E})$, there exists a smooth Ψ, tending to 1 at infinity, having the same p but a lower $\mathscr{E}$. This neighbouring state was in fact a nearby solitary wave, stretched in its s coordinate in the manner first suggested by Derrick (1964). For the lower branch, and for the entire 2D sequence, similarly stretched Ψ gave an $\mathscr{E}$ larger than the solitary wave of the same p. Although nothing can be conclusively proved from this, we conjectured that these branches are stable, a view corroborated by numerical experiments.

The time integration of a 3D state, having initially $p < p_{\min}$, strongly suggested that such states will completely disappear, by radiating their energy and momentum to infinity as sound waves. If $p > p_{\min}$, sufficiently energetic initial states appear to evolve onto the lower branch, after the energy excess has been radiated to infinity. Similarly 2D states at first above the sequence appear in time to collapse onto the sequence. It was shown explicitly in one case how a disturbance could acquire circulation as it evolved, and it was argued that this was not in conflict with the Kelvin-Helmholtz theorem. Thus the concept of circulation being a topological constraint on the motion of vortices must be revised when effects of compressibility are included. The tensor virial theorem implied by the NLS equation was deduced, but was not found useful in understanding the evolution of disturbances.

Acknowledgment

Thanks are due to the Science and Engineering Research Council for a grant (GR/C 74904) which brought the authors together.

References

Ablowitz M J and Segur H 1979 *J. Fluid Mech.* **92** 691-716
Anker D and Freeman N C 1978 *Proc. R. Soc.* A **360** 529-40
Barenghi C F, Donnelly R J and Vinen W F 1983 *J. Low Temp. Phys.* **52** 189-247
Benjamin T B 1972 *Proc. R. Soc.* A **328** 153-83
Benney P J and Roskes G J 1969 *Stud. Appl. Math.* **48** 377-85
Chandrasekhar S 1969 *Ellipsoidal Figures of Equilibrium* (New Haven, CT: Yale University Press)
Christiansen P L and Lomdahl P S 1981 *Physica* D **2** 482-94
Davey A and Stewartson K 1974 *Proc. R. Soc.* A **338** 101-10
Derrick G H 1964 *J. Math. Phys.* **5** 1252-4
Eilbeck J C 1978 *Solitons and Condensed Matter Physics* ed A R Bishop and T Schneider (Berlin: Springer)
Freeman N C 1980 *Adv. Appl. Mech.* **20** 1-37
Grant J 1971 *J. Phys. A: Gen. Phys.* **4** 695-716
Grant J and Roberts P H 1974 *J. Phys. A: Math., Nucl. Gen.* **7** 260-79
Iordanskii S V and Smirnov A V 1978 *JETP Lett.* **27** 535-6
Israeli M and Orszag S A 1981 *J. Comput. Phys.* **41** 115-35
Jones C A and Roberts P H 1982 *J. Phys. A: Math. Gen.* **15** 2599-619
Kadomtsev B B and Petviashvili V I 1970 *Sov. Phys.-Dokl.* **15** 539-41
Lee T D 1981 *Particle Physics and Introduction to Field Theory* (New York: Harwood Academic)
Makhankov V G, Litvinenko E I and Shvachka A B 1981 *Comput. Phys. Commun.* **2** 223-32
Manakov S V, Zakharov V E, Bordag L A, Its A R and Matveev V B 1977 *Phys. Lett.* **63A** 205-6
Roberts P H and Grant J 1971 *J. Phys. A: Gen. Phys.* **4** 55-72
Thomson J J 1883 *A Treatise on the Motion of Vortex Rings* (London: MacMillan)
Zakharov V E and Shabat A B 1973 *Sov. Phys.-JETP* **37** 823-8
Zakharov V E and Synakh V S 1976 *Sov. Phys.-JETP* **41** 465-8